Proceedings World Geothermal Congress 2020+1
Reykjavik, Iceland, April - October 2021

Experiment and Modeling of Heat Extraction From a Cylindrical Saturated Porous Tank With a Coaxial Open Loop

Jiashu LI, Chuanshan DAI, Fei LI, Jinhua LU, Haiyan LEI

Key Laboratory of Efficient Utilization of Low and Medium Grade Energy, Ministry of Education, 300072, TianJin, China

E-mail address, csdai@tju.edu.cn

Keywords: downhole coaxial heat exchanger; open loop; heat extraction; porous media.

ABSTRACT

Finding a clean and efficient way of mining heat from a deep geothermal reservoir is still one of the most difficult challenges in geothermal exploration. To date, borehole heat exchangers (BHE), downhole coaxial heat exchangers (DCHE), and downhole heat exchangers (DHE) can be found in some geothermal direct uses with an advantage of "no water withdrawn but heat only". In order to overcome the low heat extraction efficiency for the deep downhole coaxial heat exchanger (DCHE), a downhole coaxial open loop (DCOL) design was proposed. In this paper, the heat extraction mechanism for the DCOL was investigated experimentally at a lab scale by accounting mainly for the effects of and thermal properties of the surrounding porous medium, and inlet water temperature and flowrate, etc. In addition, a two-dimensional axisymmetric fluid flow and heat transfer model was established and solved numerically by using Lattice Boltzmann method (LBM). An extended Brinkman-Forchheimer-Darcy Whitaker model was adopted for simulating the mixed convection in porous media. Results show that the configuration of the DCOL has a larger heat extraction rate comparing with the closed loop of DCHE. The inlet temperature and circulation flowrate of the loop have also a great influence on its final heat extraction rate.

1. INTRODUCTION

One of the problems in geothermal utilization by pumping geofluids directly out of aquifers is the surface disposal, which may cause the thermal and chemical pollution on the surface environment in addition to the drawdown of groundwater level. It is well known that the best way to overcome this problem is to reinject fully the "cooled" geothermal fluid back to the same aquifer through one or more reinjection wells near the production well. However, in some cases this might not be technical feasible, such as the reinjection in some sandstone reservoirs. The actions of more pumping and less reinjection, or no reinjection, will definitely result in the decline of groundwater level year by year and increase the risk of land subsidence. Therefore, it is necessary to explore a geothermal utilization technology that has the feature of "no water withdrawn but heat only", such as the technologies of downhole heat exchanger (DHE), borehole heat exchanger (BHE) based on the closed loop from a single geothermal well.

For the geothermal development and utilization technology of "no water withdrawn but heat only", it mainly includes: single well column (Song et al. (2014)), borehole heat exchanger (BHE) (Alimonti C et al. (2018)) and downhole heat exchanger (DHE) (Lund JW (1999)). However, the single well pumping technology has not yet removed the reinjection problem. Since DHEs and BHEs do not have reinjection problems, they have been given more attentions by some geothermal researchers (Dai C et al. (2011), Lund JW and Boyd TL (2016)). The difference between DHE and BHE is that the wall of the BHE is in direct contact with the surrounding formation, and the wall of the DHE is in contact with the fluid in the well. Therefore, the BHE mainly transfers heat from the formation around the wellbore to the pipe through heat conduction, while the DHE has the geothermal water in the well, which can form natural convection to enhance heat transfer. So even considering the heat transfer temperature difference, the traditional DHEs can deliver more than one order of magnitude of heat than that of the BHE (Lund J W (1999)).

Early DHE were mainly installed in a well penetrated through a shallow geothermal aquifer, for instance, U-shaped tube or coaxial sleeve were placed in the well. In order to enhance the heat exchange capacity, a tube with an upper and lower opening installed in parallel with the U-shaped tube or the coaxial sleeve is placed below the water level in the well, which was called a convection promoter (Christopher S et al. (2012)). The shallow BHE mainly refers to a single U-tube or double U-PEX tubes installed in a drilled hole filled up with backfill. In recent years, with the advancement of well drilling technology, the deep borehole heat extraction technology has been increasingly paid attention. Considering the convenience of installation for the deep geothermal wells, the tube-in-casing or the coaxial structure was generally adopted (Kohl T et al. (2002)). That is, the cold fluid flows downward through the annular section between the inner tube and outer casing to the bottom of the well, absorbs heat from the surrounding formation along the path, and then returns back upon reaching to the bottom through the insulated inner tube to the surface.

An early field test of a deep coaxial heat exchanger was carried out in Hawaii in 1992 (Morita K et al. (1992)), and a summary of those researches related to this topic in recent years was given by Alimonti (2018). The advantage of this structure is that clean water is used as the circulating water, which can directly enter the heat pump evaporator. The disadvantage is that the closed well casing cuts off the possible mass transfer between the circulating fluid in the wellbore and the fluid in the geothermal aquifer. Therefore, the close-looped deep coaxial heat exchanger is relatively inferior to the open looped downhole heat exchanger. In order to improve the heat extraction rate for the middle-deep geothermal wells, in 2016, GEL of the United Kingdom proposed an open downhole heat transfer and heat extraction system, and successfully conducted field tests in Penzance, the southwestern part of the UK (Westaway R (2018)).

Due to the open outer casing structure, the inner pipe needs to have a deep well pump to extract geothermal water to the ground for heat exchange. In their test, the pump input power is about 7 kW and the total flow rate is 3L/s. According to the report, the outlet

temperature of returned geothermal water is 69 °C with a 2000m deep well. A peak heat output of 363 kW was achieved, (Westaway (2018)). Our research team also conducted an on-site heat extraction test in Tianjin Tanggu by using a similar open coaxial design. The experimental results show that the designed system has a good heat extraction performance. After two weeks of continuous heat extraction, a stable heat output of approximately 275 kW can be reached, which is much larger than the theoretical calculation of deep BHE using a thermal conductivity model (Dai et al. (2019)). However, the influencing factors on the heat transfer capacity of the open casing structure are yet unclear and need in-depth research.

This paper establishes a simulation experiment system to study the heat extraction characteristics of coaxial open-looped downhole (DCOL) heat exchangers in saturated aquifers, and the dynamic change of heat extracted and temperature profiles in the aquifer under different conditions. The heat extraction mechanism for the DCOL was investigated experimentally at a lab scale by accounting for the effects of geometrical parameters of the wellbore and inner tube, the hydraulic and thermal properties of the surrounding porous medium, and inlet water temperature and flowrate. In addition, a two-dimensional axisymmetric fluid flow and heat transfer model was also established and solved numerically by using Lattice Boltzmann method (LBM). An extended Brinkman-Forchheimer-Darcy Whitaker model was adopted for simulating the mixed convection in porous media.

2. EXPERIMENTAL SETUP OF THE DEEP DCOL SYSTEM

The experimental system of the downhole coaxial open loop is carried out in a cylindrical steel tank filled with small glass beads to simulate the hot water reservoir. The inner diameter of the cylindrical tank is 1000mm, and the height 1000mm. The diameters of glass beads are about 2.5mm~3mm. The outside of the tank is wrapped completely with 30mm thick plastic foam. In the center of the reservoir, there is a coaxial heat exchanger installed vertically, which constitutes an inner plastic tube of 9 mm in outer diameter and a uniformly perforated steel tube of 30 mm in inner diameter.

The experimental setup is shown as in Fig.1. The temperature measuring points are arranged at the inlet and outlet of the coaxial pipes, and some points around in the reservoir, respectively (the solid dots). There are 36 T-type thermocouples placed in three vertical layers along the depth of the well. At beginning of the experiment, the whole tank was heated by circulating hot water with a controlled temperature through a separate loop (pump 2). After the whole reservoir reached a certain constant, the circulating pump was turned off and kept for about 20 minutes in order to have a uniform and stable temperature distribution in the porous tank. The experiment can be started after confirming that the entire reservoir was in a relative static and steady thermal condition. In general, the measured temperatures inside the tanks have a temperature deviation less than 2 °C. The cold water through the DCOL was controlled by another circulation pump (pump 1), and its flow rate was measured by balance weighing method. The data acquisition of all measured temperatures was realized by Agilent 34980 recorder in real time.

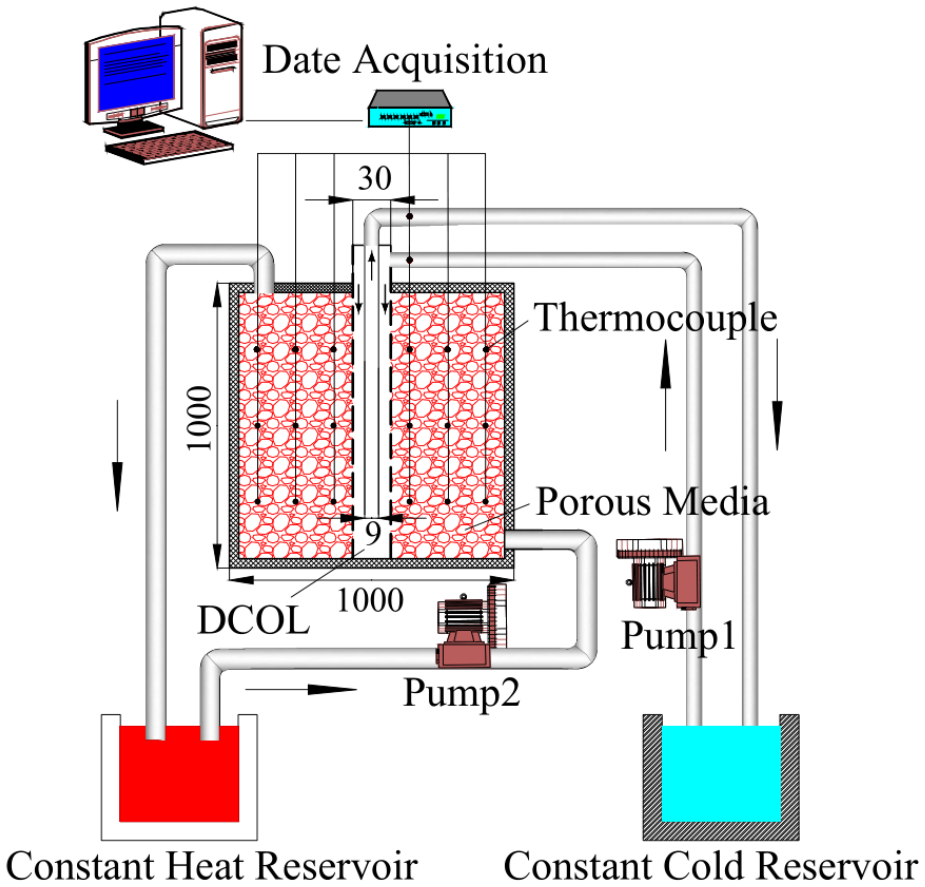

Figure 1: Experimental system for heat extraction with a downhole coaxial open loop (DCOL).

3 EXPERIMENTAL RESULTS OF THE DCOL SYSTEM

Some factors affecting the heat power of the downhole coaxial open loop were studied experimentally including working fluid flow (Qin) and inlet water temperature (Tin). The specific experimental results are as follows.

3.1 Effect of working fluid flowrate

The effect of flowrate on the heat extraction rate was studied by fixing the inlet temperature at approximately 25ºC, the initial reservoir (tank) temperature was 50° C. Three tests with various flowrates were performed. In particular, the flow rate was measured by the balance weighing method, the real flowrates for the three cases are 14.5ml/s, 18.8ml/s, 40.2ml/s, respectively. Figures 2 and 3 show the measured outlet temperatures and the heat outputs with time. It can be seen from the figure that the trends of the heat output with time are basically consistent with those of outlet temperature.

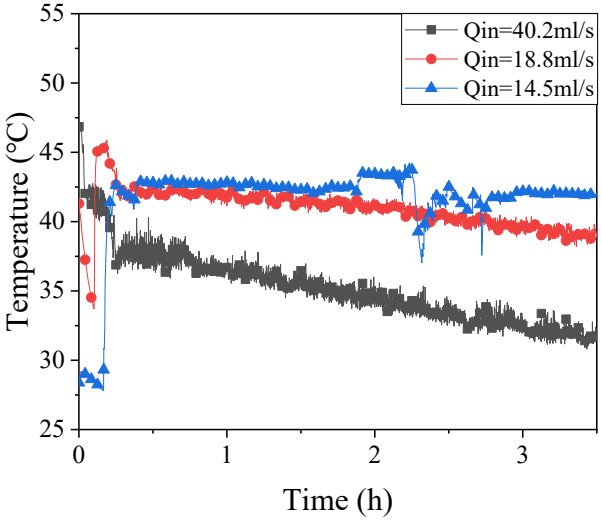

Figure 2: Effect of flow rates on outlet temperature

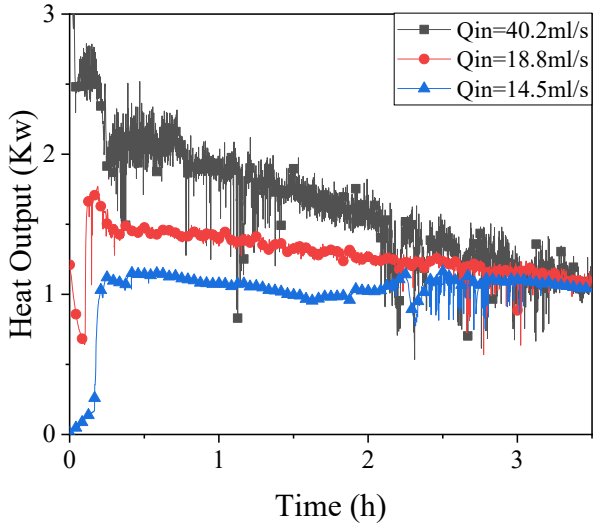

Figure 3: Effect of flow rates on heat output

As shown in Fig. 2, when the flow rate is large, the outlet temperature changes quickly with time at the beginning, and the final stabilized temperature is lower compared to those of the smaller flowrate cases. As the flow rate decreases, the outlet temperature decreases for a short period and then increases remarkably. When the flow rate increased from 14.48ml/s to 18.76ml/s, the flow rate was increased by 29% while the steady-state final temperature decreased by 6%. When the flow rate increased from 14.48ml/s to 40.22ml/s, the flow rate increased by 177% while the steady-state temperature decreased by 25%. When the flow rate is small, there is a fluctuation in the outlet temperature because the flow rate is controlled by the valve. When the flow rate is too small, the pump supply pressure is unstable resulting in no water flowing out in a few minutes at about 2 hours later.

Fig. 3 shows that the initial heat output increases with the increase of the flow rate. When the flow rate was increased from 14.48ml/s to 18.76ml/s, by 29%, the peak heat output increased by 48%. When the flow rate was increased from 14.48ml/s to 40.22ml/s, by 177%, the peak heat output increased by 136%. However, with time going on, the heat extraction rates for different flow rates tends to be the same. This is because the initial temperatures of the tank are the same, the inlet temperatures the same as well and the adiabatic boundary conditions are given for all the cases.

3.2 Effect of inlet temperature

In order to see the effect of inlet temperature on the heat extraction rate, the flow rate was kept at approximately 15ml/s, and the initial tank temperature was controlled at 50° C. The inlet temperature was varied by three cases of 8° C, 15° C, 25° C. Figures 4 and 5 show the effects of different inlet temperature on the outlet temperature and the heat output. It can be seen that the variations of the heat output and the outlet temperature with time are basically consistent. They both change quickly over time at the beginning, slow gradually, and finally are stabilized.

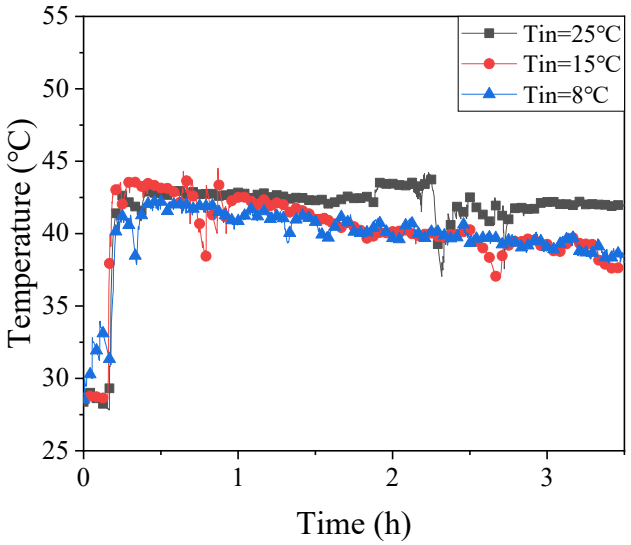

Figure 4: Effect of inlet temperature on outlet temperature

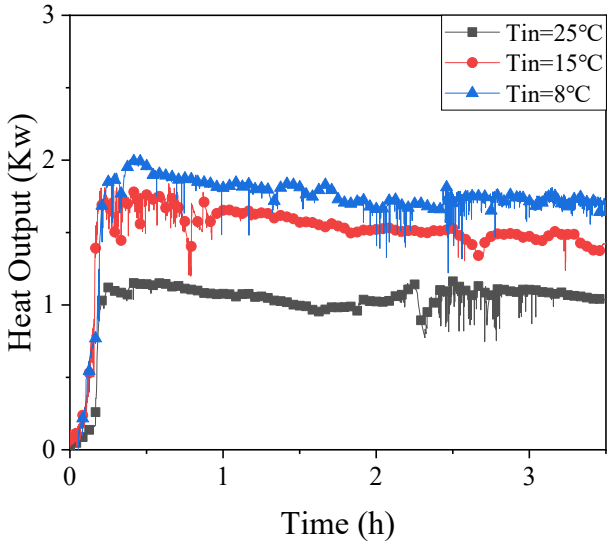

Figure 5: Effect of inlet temperature on heat output

Fig. 4 also shows that the change of inlet temperature has a small effect on the outlet temperature change at the beginning, but after a while a higher inlet temperature results in a higher outlet temperature. The outlet temperatures for the two cases of low inlet temperatures become almost the same after running 1.5 hours. When the inlet temperature decreases from 25° C to 15° C, by 40%, the outlet temperature decreases by 8.2% after running about 3.5 hours. When the inlet temperature decreases from 25° C to 8° C, by 68%, with the outlet temperatures decreases by about 9.2% after 3.5 hours. As shown in Fig.5, the heat output decreases in general as the inlet temperature increases. When the inlet temperature decreases from 25° C to 8° C, the peak heat output increases by 41.3% in this case.

4. LATTICE BOLTZMANN METHOD ANALYSIS OF DCOL

4.1 Mathematic model of DHE

A 2D axisymmetric fluid flow and heat transfer model was used in the simulation. The interface condition between the wellbore with the porous formation was coupled with the forced convection heat transfer of the annular section (flowing from top to bottom) and inner pipe (flowing from bottom to top), as shown in Fig. 6. The governing equations of mass continuity, momentum, and energy in porous media are given, respectively, as follows,

$$\frac{\partial}{\partial x}(\rho u_x)+\frac{1}{r}\frac{\partial}{\partial r}(r\rho u_r)=0 \tag{1}$$

$$\frac{\partial(\rho u_x)}{\partial t}+\frac{1}{\varepsilon}\frac{\partial}{\partial x}(\rho u_x u_x)+\frac{1}{r\varepsilon}\frac{\partial}{\partial r}(r\rho u_x u_r)=-\frac{\partial(\varepsilon p)}{\partial x}+\rho\upsilon_e\left[\frac{\partial}{\partial x}\left(\frac{\partial u_x}{\partial x}\right)+\frac{1}{r}\frac{\partial}{\partial r}\left(r\frac{\partial u_x}{\partial r}\right)\right]+\rho F_x \tag{2}$$

$$\frac{\partial(\rho u_r)}{\partial t}+\frac{1}{\varepsilon}\frac{\partial}{\partial x}(\rho u_x u_r)+\frac{1}{r\varepsilon}\frac{\partial}{\partial r}(r\rho u_r u_r)=-\frac{\partial(\varepsilon p)}{\partial r}+\rho\upsilon_e\left[\frac{\partial}{\partial x}\left(\frac{\partial u_r}{\partial x}\right)+\frac{1}{r}\frac{\partial}{\partial r}\left(r\frac{\partial u_r}{\partial r}\right)-\frac{u_r}{r^2}\right]+\rho F_r \tag{3}$$

$$\frac{\partial T}{\partial t}+u_x\frac{\partial T}{\partial x}+u_r\frac{\partial T}{\partial r}=\alpha\left[\frac{\partial}{\partial x}\left(\frac{\partial T}{\partial x}\right)+\frac{1}{r}\frac{\partial}{\partial r}\left(r\frac{\partial T}{\partial r}\right)\right] \tag{4}$$

where u_r and u_x are radial velocity and axial velocity, respectively. p is the pressure, υ_e is effective kinetic viscosity, α is thermal diffusion coefficient. $F = (F_x, F_r)$ represents the total body force due to the presence of porous medium and other external force, and is given by

$$F_\psi=-\frac{\varepsilon\upsilon}{K}u_\psi-\frac{\varepsilon F_\varepsilon}{\sqrt{K}}|u|u_\psi+\varepsilon G,(\psi=x,r) \tag{5}$$

where υ is the kinetic viscosity of fluid and G is the body force. The geometric function F_ε and the permeability K of the porous medium are related to the porosity ε, and can be expressed as:

$$F_\varepsilon=\frac{1.75}{\sqrt{150\varepsilon^2}}\qquad K=\frac{\varepsilon^3 {d_p}^2}{150(1-\varepsilon)^2} \tag{6}$$

where d_p is the diameter of a solid particle.

4.2 LBE model

In this study, the Lattice Boltzmann method (LBM) was used for simulating the axisymmetric thermal flows through porous medium, as proposed by Fumei Rong (2010). In this model, two distribution functions were adopted for simulating, respectively, the fluid flow and temperature in porous media.

The evolution equation for axisymmetric thermal flow through porous medium can be written as:

$$f_i(\boldsymbol{x}+\boldsymbol{x}\Delta t,t+\Delta t)-f_i(\boldsymbol{x},t)=-\frac{1}{\tau_f}\left[f_i(\boldsymbol{x},t)-f_i^{eq}(\boldsymbol{x},t)\right]+\delta t(1-\frac{1}{2\tau_f})F_i(\boldsymbol{x},t) \tag{7}$$

where $f_i(\boldsymbol{x},t)$ is volume-average distribution function with velocity $\boldsymbol{c}_i$ at position $\boldsymbol{x}$ and time t, τ_f is non-dimensional relaxation time related to viscosity. The exact expressions of the equilibrium distribution function $f_i^{eq}(\boldsymbol{x},t)$ and forcing term $F_i(\boldsymbol{x},t)$ can be found in Fumei Rong (2010).

For the temperature field represented by another distribution function of h follows an evolution of:

$$h_i(\boldsymbol{x}+\boldsymbol{x}\Delta t,t+\Delta t)-h_i(\boldsymbol{x},t)=-\frac{1}{\tau_h}\left[h_i(\boldsymbol{x},t)-h_i^{eq}(\boldsymbol{x},t)\right]+\delta t H_i(\boldsymbol{x},t) \tag{8}$$

where τ_h is non-dimensional relaxation time related to thermal diffusion coefficient. The exact expressions of the equilibrium distribution function $f_i^{eq}(\boldsymbol{x},t)$ and forcing term $F_i(\boldsymbol{x},t)$ can be found in Fumei Rong (2010).

The fluid density ρ, temperature T and velocity $\boldsymbol{u}$ are, respectively, computed by:

$$\rho=\frac{1}{r}\sum f_i(\boldsymbol{x},t) \tag{9}$$

$$T=\frac{1}{r}\sum h_i(\boldsymbol{x},t) \tag{10}$$

$$\boldsymbol{u}=\frac{\boldsymbol{v}}{d_0+\sqrt{d_0^2+d_0|\boldsymbol{v}|}} \tag{11}$$

where $\boldsymbol{v}$ is an intermediate speed variable can be derived from:

$$\rho\boldsymbol{v}=\sum c_i f_i(\boldsymbol{x},t)+\frac{\delta t}{2}r\rho\epsilon G+\frac{\delta t}{2}\rho R_g T\delta_{\alpha r} \tag{12}$$

and d_0 d_1, have the following form:

$$d_0 = \frac{r^2+\tau_f\delta_t R_g T\delta_{ar}}{r} + r\epsilon\frac{\delta t}{2}\frac{\mu}{K}, d_1 = r\epsilon\frac{\delta t}{2}\frac{F_\varepsilon}{\sqrt{K}} \quad (13)$$

4.3 Boundary conditions

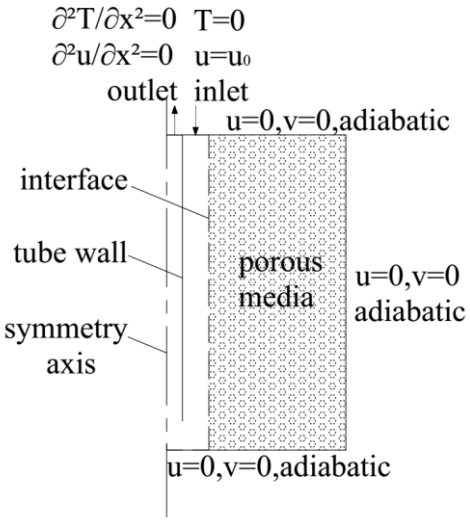

Figure 6: The model of DCOL

For the geothermal well, the inlet temperature is fixed at a constant temperature and the outlet temperature is given by extrapolating the outlet boundary condition. At the bottom, water flows from the outer annular into the inner tube and is considered as an adiabatic boundary condition. At the inner tube wall, the heat fluxes on the left and right sides are given to be the same.

$$T_{f,in} = 0, \qquad U_{f,in} = u_0 \quad (14)$$

$$\frac{\partial^2 T_{f,out}}{\partial Z^2} = 0, \qquad \frac{\partial^2 U_{f,out}}{\partial Z^2} = 0 \quad (15)$$

$$\frac{\partial T_{f,bottom}}{\partial Z} = 0, \qquad U_{f,bottom} = 0 \quad (16)$$

$$\mathrm{K}_f\frac{\partial T_{f,left}}{\partial r} = \mathrm{K}_f\frac{\partial T_{f,right}}{\partial r} = \lambda_{wall}\frac{T_{f,right}-T_{f,left}}{\delta_{wall}} \quad (17)$$

For the geothermal reservoir, the bottom, top and right walls are assumed to be under adiabatic and no-slip conditions.

$$\frac{\partial T_{s,bottom\&top\&right}}{\partial Z} = 0, \qquad U_{s,bottom\&top\&right} = 0 \quad (18)$$

At the interface between open fluid and porous medium, the two sets of equations are coupled by the following matching conditions at the porous/fluid layer interface (Ochoatapia Ja (1998)).

$$u_t|_{porous} = u_t|_{fluid}, \qquad u_n|_{porous} = u_n|_{fluid} \quad (19)$$

$$\frac{1}{\varepsilon}\frac{\partial u_t}{\partial n}|_{porous} - \frac{\partial u_t}{\partial n}|_{fluid} = \frac{\beta}{\sqrt{K}}u_t|_{interface} + \frac{\beta_1}{\nu}{u_t}^2|_{interface} \quad (20)$$

$$\frac{1}{\varepsilon}\frac{\partial u_n}{\partial n}|_{porous} - \frac{\partial u_n}{\partial n}|_{fluid} = 0 \quad (21)$$

$$\mathrm{K}_f\frac{\partial T_f}{\partial r} = \mathrm{K}_{eff}\frac{\partial T_s}{\partial r} \quad (22)$$

where u_t is the velocity component parallel to the interface and u_n is the velocity component perpendicular to the interface. K is the permeability coefficient, ν is the kinematic viscosity of the fluid, and β and β_1 are the stress jump parameters. In the current study, the values of the two parameters are -1.0~+0.7.

4.4 Numerical results

4.4.1 Natural convection in a vertical porous annulus

In this section, we will validate the proposed model by simulating the flows with boundary conditions and initial temperature the same as those reported in Fumei Rong (2010). Figure 7 shows the comparison of the present results for temperature filed and streamline distributions with those of the literature (Fumei Rong (2010)). As shown in Figure 7, (a) the obtained temperature and streamlines are in agreement with those of Fumei Rong (Fig. 7(b)). The porous medium was composed of glass spheres with diameter d=22.25 mm and filled with water, the gap between two cylinders was $L=r_0-r_i=123.85$ mm. The aspect ratio (X/L) and radii ratio (r_0/r_i) set to be 1 and 5.338, and $\varepsilon=0.431$ and Pr=7, respectively. In the present study, the parameter Ra* is defined as Ra* = RaDa, the Da=0.000053 and Ra*=2000 for this case.

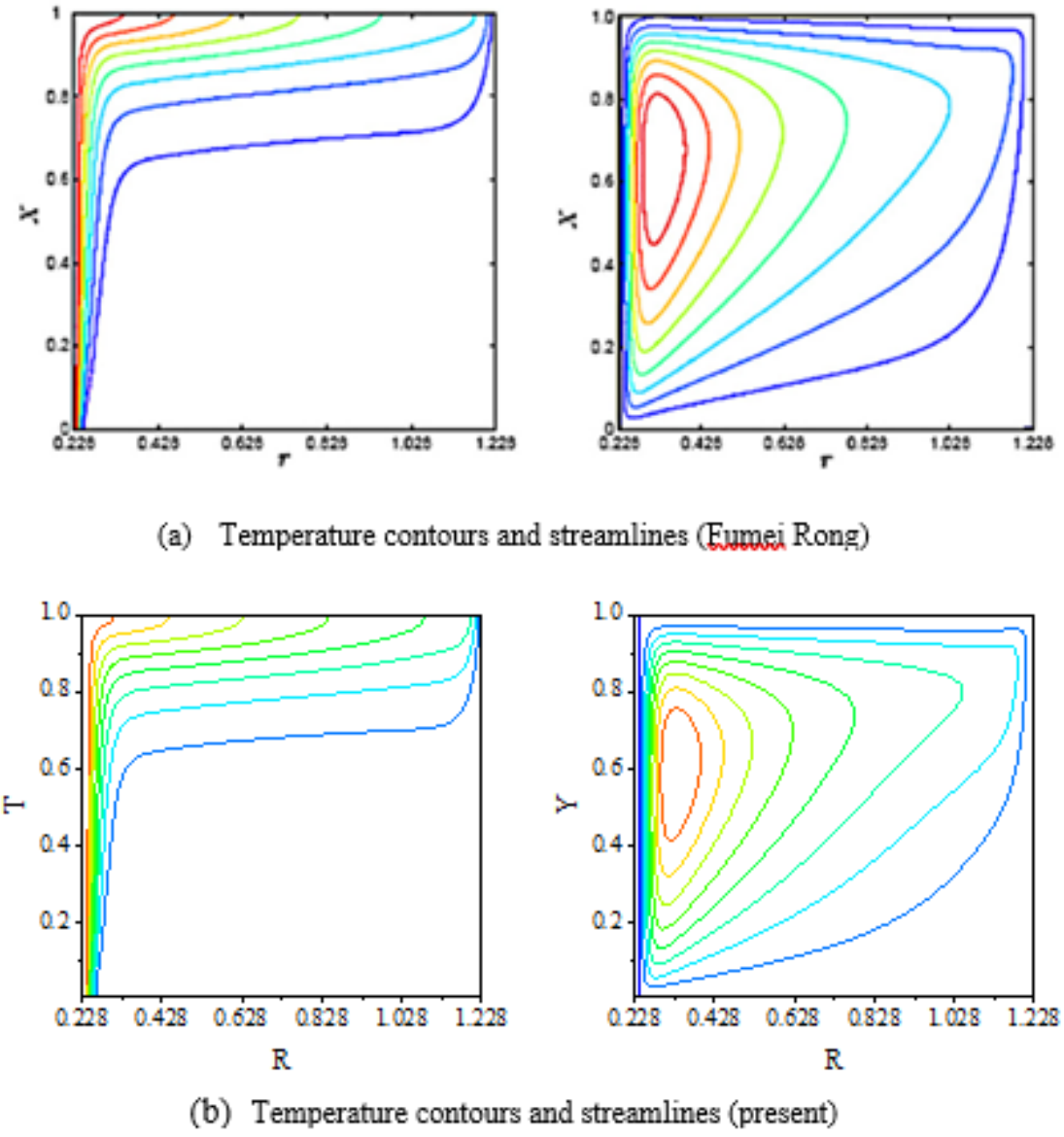

Figure 7: comparison of the present results for temperature filed and streamline with other literature

4.4.2 Comparison of simulated and experimental results

We compared the outlet temperatures from the experimental results with those from the simulation. The experiment was performed at the inlet temperature of 25° C, the flow rate approximately of 40ml/s, and the initial tank temperature of 68° C, 60° C, 50° C, respectively. The dimensionless parameters were as follows: Prandtl number of 7, Darcy number of 4.3×10^{-7}, Reynolds number of 1500, porosity of 0.4. At initial temperature of 68° C, 60° C, 50° C, the Rayleigh number corresponds to 6.8×10^{8}, 4.6×10^{8}, 3.0×10^{8}, respectively.

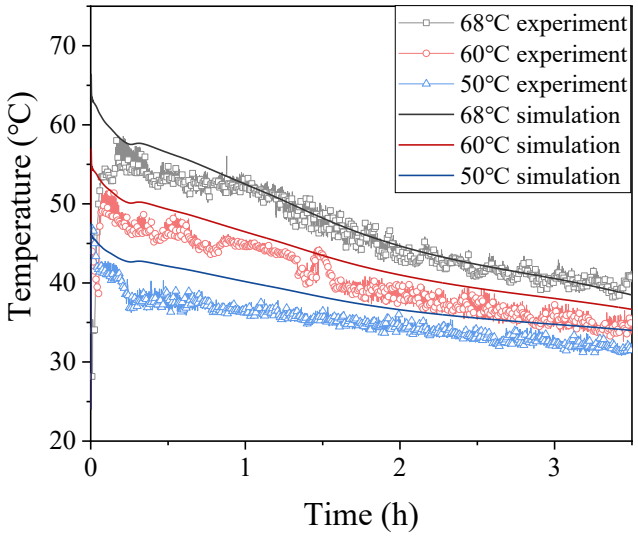

Figure 8: The measured and simulated outlet dimensionless temperatures with time

As shown in Fig.8, the simulation results have the same trends as the experimental results, and there is an obvious significant temperature drop at the initial stage, after which the temperature decrease tends to be slow. There is a large deviation for the experimental outlet temperature with that of the simulation. However, the calculated temperature for the three cases are in general, consistent with the experimental curves. It seems that the deviation for the simulated outlet temperature comparing with the experimental data becomes larger with decreasing tank temperature. This may due to the input data errors, such as the heat transfer coefficient K_f between the outer tube and the inner tube, the thermal physical properties of glass spheres and permeability etc. In addition, the water viscosity and thermal diffusivity are temperature dependent, which results in errors between the theoretically calculated Rayleigh number and the actual Rayleigh number.

4. DISCUSSION AND CONCLUSIONS

In this paper, an experimental setup at a lab scale for modeling the heat extraction performance of a deep coaxial open loop downhole heat exchanger in a porous aquifer was established. Some experiments were carried out at different inlet water temperature and different circulating flowrate. The influences of these parameters on the heat output are obtained.

The results indicate that: (1) as the flow rate decreases, the peak outlet temperature has a hysteresis. However, as time goes by, the extracted heat at different flow rates tends to be the same. When the flow rate increases from 14.48ml/s to 18.76ml/s, i.e. the flow rate increase by 29%, the peak heat output increases by 48%. When the flow rate increases from 14.48ml/s to 40.22ml/s, the flow rate increased by 177% while the peak heat output increased by 136%. (2) For various inlet temperatures, the outlet temperatures for the two cases of low inlet temperatures become almost the same after running 1.5 hours. When the inlet temperature decreases from 25° C to 15° C, the peak heat output increases by 35.9%. When the flow rate decreases from 25° C to 8° C, the peak heat output increases by 41.3%. (3) The simulation results have the same trend as the experimental results, however, there are a large differences between experiments and simulations in the initial state. There are still errors between the experimental results and simulation results, when the system became stabilized at low initial temperatures. Both experiments and simulations are needed to be performed in detail in the future.

REFERENCES

Alimonti C, Soldo E, Bocchetti D, Berardi D: The wellbore heat exchangers A technical review, *Renewable Energy*, **123,** (2018), 353-381.

Dai C, Xie S, Lei H: A case study of space heating using a downhole heat exchanger in China, *GRC Transaction*, **35**, (2011), 1077-1080.

Dai C, Chen Y: Classification of shallow and deep geothermal energy resources, *GRC Bulletin*, **32**, (2008), 317-320.

Dai C, Li Jiashu, Shi Y., et al.: An experiment on heat extraction from a deep geothermal well using a downhole coaxial open loop design, *Applied Energy*, (2019).

Christopher S, Andy B, Sadiq JZ: Improving the performance of the down-hole heat exchanger at the AlpineMotel, Rotorua, New Zealand, *Geothermics*, 2012, 44:1-12.

Kohl T, Brenniand R, Eugster W: System performance of a deep borehole heat exchanger, *Geothermics*, **31**, **(**2002), 687-708.

Lund JW: Large Downhole Heat Exchanger in Turkey and Oregon, *GHC Bulletin*, (1999), 17-19.

Lund JW, and Boyd TL: Direct utilization of geothermal energy 2015 worldwide review, *Geothermics*, **60, (**2016), 66-93.

Lund JW: Examples of Individual Downhole Heat Exchangers Systems in Klamath Falls, *GHC Bulletin*, **3**, (1999), 20-24.

Morita K, Bollmeier K S, Mizogami H: An experiment to prove the concept of the downhole coaxial heat exchanger (DCHE) in Hawaii, *GRC Transactions*, **16**, (1992), 9-16.

Ochoatapia, Ja and S. Whitaker: Momentum jump condition at the boundary between a porous medium and a homogeneous fluid: inertial effect, *Journal of Porous Media*, **1**, (1998), 201-217.

Rong, Fumei , et al : A lattice Boltzmann model for axisymmetric thermal flows through porous media, *International Journal of Heat and Mass Transfer*, **53**, (2010), 5519-5527.

Wei Song, N. I. Long, and Y. Yang: Characteristics of single well systems in different initial aquifer temperatures, *Journal of Harbin Engineering University*, **3,** (2014), 342-346.

Westaway R: Deep Geothermal Single Well heat production: Critical appraisal under UK conditions, *Quarterly Journal of Engineering Geology and Hydrogeology*, **51**, (2018), 424-449.